



NRC Publications Archive Archives des publications du CNRC

Low thrombogenicity coating of nonwoven PET fiber structures for vascular grafts

Dimitrievska, Sashka; Maire, Marion; Diaz-Quijada, Gerardo A.; Robitaille, Lucie; Aji, Abdellah; Yahia, L'Hocine; Moreno, Maria; Merhi, Yahye; Bureau, Martin N.

This publication could be one of several versions: author's original, accepted manuscript or the publisher's version. / La version de cette publication peut être l'une des suivantes : la version prépublication de l'auteur, la version acceptée du manuscrit ou la version de l'éditeur.

For the publisher's version, please access the DOI link below. / Pour consulter la version de l'éditeur, utilisez le lien DOI ci-dessous.

Publisher's version / Version de l'éditeur:

<https://doi.org/10.1002/mabi.201000390>

Macromolecular Bioscience, 11, 4, pp. 493-502, 2011-01-21

NRC Publications Record / Notice d'Archives des publications de CNRC:

<https://nrc-publications.canada.ca/eng/view/object/?id=e1c5bdba-06ee-4e99-9f88-82cbea296866>

<https://publications-cnrc.canada.ca/fra/voir/objet/?id=e1c5bdba-06ee-4e99-9f88-82cbea296866>

Access and use of this website and the material on it are subject to the Terms and Conditions set forth at

<https://nrc-publications.canada.ca/eng/copyright>

READ THESE TERMS AND CONDITIONS CAREFULLY BEFORE USING THIS WEBSITE.

L'accès à ce site Web et l'utilisation de son contenu sont assujettis aux conditions présentées dans le site

<https://publications-cnrc.canada.ca/fra/droits>

LISEZ CES CONDITIONS ATTENTIVEMENT AVANT D'UTILISER CE SITE WEB.

Questions? Contact the NRC Publications Archive team at

PublicationsArchive-ArchivesPublications@nrc-cnrc.gc.ca. If you wish to email the authors directly, please see the first page of the publication for their contact information.

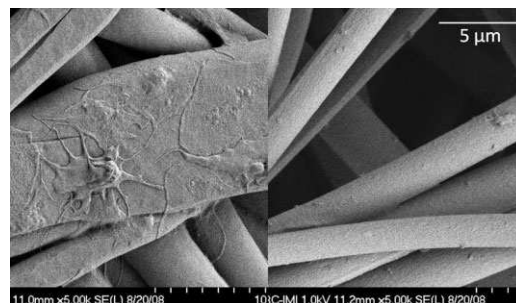
Vous avez des questions? Nous pouvons vous aider. Pour communiquer directement avec un auteur, consultez la première page de la revue dans laquelle son article a été publié afin de trouver ses coordonnées. Si vous n'arrivez pas à les repérer, communiquez avec nous à PublicationsArchive-ArchivesPublications@nrc-cnrc.gc.ca.



Low Thrombogenicity Coating of Nonwoven PET Fiber Structures for Vascular Grafts

Sashka Dimitrievska, Marion Maire, Gerardo A. Diaz-Quijada, Lucie Robitaille, Abdellah Ajji, L'Hocine Yahia, Maria Moreno, Yahye Merhi, Martin N. Bureau*

Vascular PET grafts (Dacron) have shown good performance in large vessels (≥ 6 mm) applications. To address the urgent unmet need for small-diameter (2–6 mm) vascular grafts, proprietary high-compliance nonwoven PET fiber structures were modified with various PEG concentrations using PVA as a cross-linking agent, to fabricate non-thrombogenic mechanically compliant vascular grafts. The blood compatibility assays measured through platelet adhesion (SEM and mepacrine dye) and platelet activation (morphological changes, P-selectin secretion, and TXB2 production) demonstrate that functionalization using a 10% PEG solution was sufficient to significantly reduce platelet adhesion/activation close to optimal literature-reported levels observed on carbon-coated ePTFE.



Introduction

Synthetic vascular grafts, including the ones based on polyethylene terephthalate (PET), exhibit high failure-rates

due to thrombosis and compliance mismatch-induced myointimal hyperplasia, especially in small diameter applications (< 6 mm).^[1,2] An important early step in synthetic graft failure is the platelet adhesion and thrombosis, occurring despite the use of antiplatelet and anticoagulant therapies reinforcing the inherent thrombogenicity of synthetic materials.^[3,4] Many years of intensive research on biomaterials have not yet produced a synthetic material proven suitable for the latter application. To reduce platelet adhesion, coatings of the internal synthetic surface have included grafting polysaccharides or hydrophilic polymers to suppress platelet and protein adhesion on the luminal side, thereby increasing the graft hemocompatibility.^[5–10]

Previously, we developed melt-blown nonwoven PET porous fiber structures, with controllable fiber diameter and pore size allowing an optimized fiber density, size, and inter-fiber pore size for growth and attachment of vascular cells.^[2,11,12] The nonwoven PET fiber structures with optimized porosity allow faster endothelialization with higher cellular confluence than commercially available polytetrafluoroethylene (PTFE) and knitted Dacron. As shown in the literature, the amount of cellular infiltration which correlates with thrombus free area is greatest for an

M. N. Bureau, S. Dimitrievska, M. Maire, G. A. Diaz-Quijada, L. Robitaille
Industrial Materials Institute, National Research Council Canada, 75 de Mortagne, Boucherville, QC, J4B 6Y4, Canada
Fax: (450) 641-5105; E-mail: Martin.Bureau@cnrc-nrc.gc.ca
M. Maire, L'H. Yahia
Laboratoire d'Innovation et d'Analyse de Bioperformance (LIAB), École Polytechnique de Montréal, 2500 Chemin de Polytechnique, Montréal, QC, H3T 1J4, Canada
A. Ajji
Department of Chemical Engineering, École Polytechnique de Montréal, 2500 Chemin de Polytechnique, Montréal, QC, H3T 1J4, Canada
M. Moreno
Institute for Biological Sciences, National Research Council Canada, Bldg-M54 1200, Montreal Road, Ottawa, ON, K1N 0R6, Canada
Y. Merhi
Montreal Heart Institute, 5000, Bélanger Street, Montréal, QC, H1T 1C8, Canada

intermediate pore size scaffold with consequently little evidence of any endothelialization in PTFE (no porosity) and patchy endothelial layer after humans implantation with knitted Dacron (which is more porous than PTFE).^[13] As previously reported by our group, the nonwoven PET fiber structures with pore size range 1–20 μm proved to be the optimal structures for vascular cell growth and adhesion suggesting that they will also best support autologous stem cells.^[2] Additionally, our nonwoven PET 3D tubular grafts show bio-mechanical compliance dynamically comparable to the mechanical properties of native internal mammary artery and saphenous veins.^[2] There are two important advantages of this off-the-shelf vascular conduit over the various cell based decellularized tissue engineered grafts. The first is the avoidance of 6 to 9 month culture time associated with high costs. The second is the averting of the degradation of the mechanical properties of the tissue engineered vessels associated with cellular changes in human smooth muscles cells caused by blood vessels culture time.^[14] Beyond the immediately targeted small diameter vascular grafts replacement, the nonwoven PET scaffold is also an attractive candidate in regenerative medicine and tissue engineering as its mechanical properties are custom tailorable to airway conduits or vascular modulus^[1–3] offering properties equivalent to the replacing tissue. The nonwoven PET scaffold could also be potentially used as an airway replacement, as currently attempts to replace large airways are hindered by the match of ideal mechanical properties and absence of antigenicity requisites, both of which are inherent in the nonwoven PET scaffold.^[15]

In this work, we have developed an efficient method for surface modification of the nonwoven PET scaffolds with polyethylene glycol (PEG), motivated by the properties of PEG in reducing platelet adhesion and its FDA approval as a biomedical surfactant.^[16,17] Additionally, PEG-coated medical devices prevent non-specific protein adhesion which reduces immune and inflammatory responses, while PEG macromer chemistry versatility facilitates the incorporation of chemical and physical cues for stem cell adhesion and controlled differentiation.^[18] The marriage of advanced PEG synthetic chemistry with the current stem cell knowledge has led to a matrix that mimics the stem cell microenvironment.^[18,19] The PET surface modification process (Figure 1) in this work consists of two components: a poly(vinylamine) (PVA) backbone that acts a crosslinker,

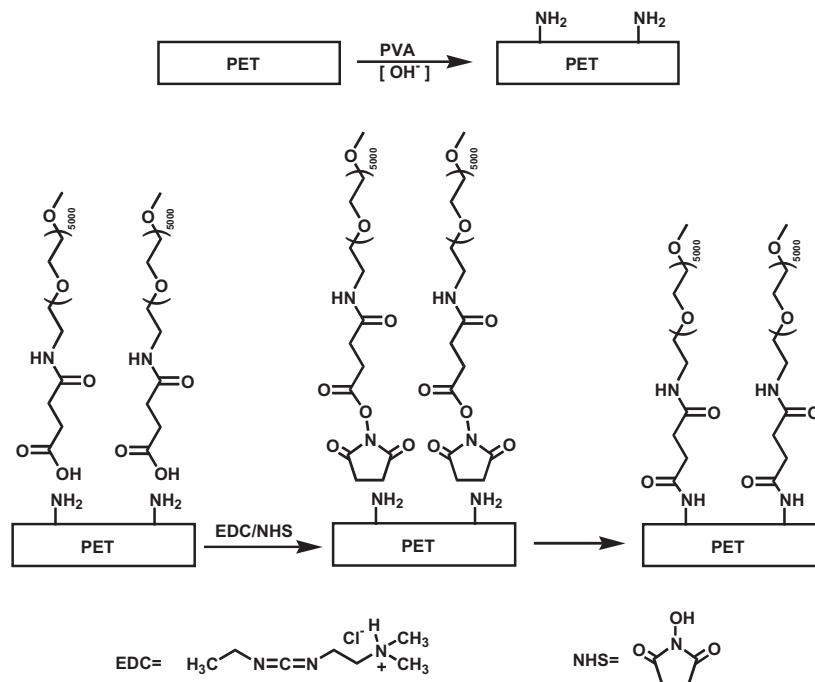


Figure 1. Schematic representation of the strategy employed for the sequential surface modification of nonwoven PET fibers with poly(vinylamine) (PVA) and PEG.

and a PEG outer layer. The first step involves the reaction of PVA with PET where PVA nitrogens nucleophilically attack the PET ester groups forming amide linkages. Subsequently, a PEG derivative that possesses a carboxylic acid group is grafted onto the amino-modified PET fibers in the presence of *N*-(3-Dimethylaminopropyl)-*N'*-ethylcarbodiimide (EDC) and *N*-hydroxysuccinimide (NHS). The selection of PVA for the PEG surface modification of PET allows enhanced control over other methods based on plasma and photochemical treatment, while avoiding the potentially pathogenic or immunoreactive biological materials inherent in the extracellular matrix (ECM) proteins. The choice of PEG was also motivated by its excellent water solubility, amphiphilicity, and stability under shear stress.^[16,17]

In addition to their known platelet repelling properties, PEG-based materials can also be resistant to the adhesion of other cell types. In other words PEG-coated biomaterials may be modulated to present a “blank slate” in terms of the biological cell interactions with the luminal side of grafts.^[16] However no conclusive ideal PEG graft densities are suggested in literature for the optimal prevention of platelet adsorption. In this study, we compare the effect of grafting different PEG concentrations on the resulting thrombogenicity of our previously developed and optimized PET nonwoven structures. The surface modifications of the fibers are characterized by X-ray photoelectron spectroscopy (XPS), and their thrombogenic potential through platelet adsorption/activation, while cell adhesion

is characterized by both EC adhesion, and viability studies (propidium iodide).

Materials and Methods

Nonwoven PET Structures

The nonwoven fiber structures were produced from a neat PET grade (Dupont, Wilmington, DE, USA) with an inherent viscosity of $1 \text{ cm}^3 \cdot \text{g}^{-1}$ using a melt-blowing process. Briefly, this process consisted of extruding PET through a multi-hole die (grid of 230 holes of $300 \mu\text{m}$ in nominal diameter). Extruded strands of PET were blown by hot air at very high speed (close to the speed of sound) through a narrow gap sideways of the die, which allowed for fiber stretching at various levels depending of the flow rate of the molten polymer. Resulting veils of nonwoven fibers were then used to fabricate the nonwoven structures by stacking several fiber veils onto a metallic plate. The plate was then inserted into an autoclave with controlled temperature for consolidation for an optimum time (patent pending). The mechanical properties of these structures were presented in ref.^[2] Their compliance, measured on tubular structures, was $8.4 \pm 1.0 \times 10^{-2} \% \text{ mmHg}^{-1}$, very similar to those reported for a variety of human arteries ($\approx 8 \times 10^{-2} \% \text{ mmHg}^{-1}$) and about seven- and eight-fold higher than those obtained with commercial Dacron grafts or ePTFE grafts, respectively.

Chemical Modification of Nonwoven PET Structures with PVA/PEG

Potassium chloride, 1,4-dioxane, sodium hydroxide, methanol, EDC (hydrochloride), NHS, ethanolamine, phosphate buffer saline (PBS), and boric acid were purchased from Sigma Aldrich (Canada). Poly(vinylamine) hydrochloride was purchased from Polysciences Inc. (USA). $\text{CH}_3\text{O}-\text{PEG}-\text{NHCO}-\text{CH}_2-\text{CH}_2-\text{COOH}$ (M_w 5000) was obtained from Rapp Polymere (Germany).

Surface functionalization of PET fibers was accomplished in two steps directly on the nonwoven PET structures. The first step involved the amino-modification of 2D nonwoven PET fibers on disk specimens that had a 10 mm diameter which were prewashed in successive baths of water (milli-Q), methanol, and water. The reaction was carried out with $100 \mu\text{L}$ of a 750 mM aqueous solution of poly(vinylamine) hydrochloride in a mixture of 1 mL buffer containing 0.1 M NaOH and 0.1 M KCl and $400 \mu\text{L}$ of 1,4-dioxane. Each sample was sonicated for 20 min and allowed to react at 70°C for 24 h in a closed Teflon container in a water bath. Samples were rinsed with water, ethanol, and water and subsequently dried under a stream of nitrogen for a few seconds.

The second step of the surface modification process involved grafting a carboxylic acid-modified PEG deriva-

tive. This was accomplished in the presence of a carbodiimide such as EDC and NHS. In this case, the NHS ester of the PEG derivative is initially formed, followed by its reaction with the amino groups present of the PVA-modified fibers (schematically described in Figure 1). The effect of the PEG solution concentration during the reaction was studied. To this end, the reaction was carried out with solutions containing 5, 7.5, 10, and 15% ($\text{mg} \cdot \mu\text{L}^{-1}$) as described in Table 1. At the end of the 24 h functionalization process, the reaction was quenched with $400 \mu\text{L}$ of a 1 M ethanolamine solution (pH 9.5) which was allowed to react for 30 min. Samples were washed with water, ethanol, and water and subsequently dried under a stream of nitrogen for a few seconds.

XPS Analysis of Pristine and Modified Nonwoven PET Structures

Pristine and surface-modified nonwoven PET fibers were characterized with XPS. Spectra were acquired on a PHI-5500 spectrometer (Physical Electronics) using monochromatized Al $K\alpha$ radiation ($h = 1486.6 \text{ eV}$) from an anode operating at 13 kV and 300 W. The operating system pressure during the scans was between 1 and 5×10^{-9} Torr. The analysis area was $0.8 \times 2 \text{ mm}^2$. For each sample, the survey spectra (0–1400 eV) were recorded at pass energy of 29.35 eV and for the high-resolution scans for the elements of interest at 11.75 eV. The eV/step of the spectrometer was 0.5 eV for survey scans and 0.1 eV for high-resolution scans. All spectra have been corrected for sample charging, with the adventitious C 1s peak (284.6 eV) used as internal reference.

Thrombogenic Potential of Nonwoven PET Structures

The thrombogenic potential of the chemically modified nonwoven PET structures was assayed through human platelet adhesion, morphological changes, and activation, after their contact with the PET structures ($n = 6$). In all biocompatibility assays we included the two most commonly used commercial vascular grafts: ePTFE (IMPRA Carboflo, 6 mm, Bard Peripheral Vascular Inc, Tempe, AZ USA) and Dacron (Hemashield Platinum, Woven Double Velour, 6 mm, Boston Scientific Medi-Tech, Wayne, NJ USA).

Table 1. Preparation of solutions for the PEG functionalization of PVA-modified PET fibers.

| [PEG \approx COOH] % ($\text{mg} \cdot \mu\text{L}^{-1}$) | 5% | 7.5% | 10% | 15% |
|---|-----|------|-----|-----|
| PEG \approx COOH (mg) | 45 | 67.5 | 90 | 135 |
| EDC (mg) | 24 | 36 | 48 | 72 |
| NHS (mg) | 6 | 9 | 12 | 18 |
| Borate buffer (μL) | 900 | 900 | 900 | 900 |

Both commercial grafts were used as controls in comparing the thrombogenicity of the chemically modified nonwoven PET structures. This research received the approval of the Research Ethics Committee of the Montreal Heart Institute (Montreal, QC) and of the ethics standards of the National Research Council of Canada.

Platelet Isolation and Labeling

Isolation and preparation of human platelets were conducted as described previously.^[20] Fresh human blood from healthy donors containing acid citrate/dextrose (ACD) as anticoagulant was centrifuged at 1800 rpm for 15 min to obtain platelet-rich plasma (PRP), which was subsequently centrifuged to obtain platelet poor plasma (PPP) and platelets were then suspended in 5 mL of EDTA containing $1 \mu\text{g} \cdot \text{mL}^{-1}$ of prostacyclin (PGI_2) (Sigma–Aldrich), and incubated with $300 \mu\text{Ci}$ of ^{51}Cr during 40 min, followed by a centrifugation at 2000 rpm for 8 min. The supernatant was removed and platelets were suspended in PPP and adjusted to 250×10^6 platelets mL^{-1} using a cell counter (Coulter Act Diff, Beckman Coulter, Canada).

Platelet Adhesion on Vascular Graft Material

The platelet adhesion on the nonwoven PET structures (pristine and functionalized), and reference grafts was performed in static platelets adhesion assay as per the protocol previously developed and described.^[21] Briefly, the structures were washed in saline solution (0.9% sodium chloride irrigation USP, Hospira Healthcare Corporation, Montreal) placed in 24-well plates with 1 mL of PRP and incubated in PRP during 1 h under gentle agitation. The structures were gently washed in saline solution to remove non-adherent platelets leaving attached and activated platelets for quantification of platelets adhesion to structures. The levels of radiolabeled platelets were counted in a gamma counter (1470 WIZARD Wallac). Platelet adhesion per surface area of each graft was calculated, as described previously.^[21]

Fluorescent Counting of Platelets

Platelets were incubated with the PET structures (pristine and functionalized), and reference grafts washed two times in PBS and then incubated in tissue fix solution for 45 min. Samples were placed in mepacrine solution (10 mM) during 90 min, and observed through a confocal microscope (Carl Zeiss LSM 510).

SEM Observation of Platelet–Vascular Graft Interactions

The platelets co-incubated nonwoven PET structures (pristine and functionalized) and reference grafts were

washed twice with PBS and fixed with 1% glutaraldehyde, for 1 h at room temperature, then overnight at 4°C . The samples were rinsed with PBS for 30 min and dehydrated through a series of graded alcohol solutions. The specimens were air-dried overnight and the dry cellular constructs were finally sputter-coated with palladium and observed under the SEM (SEM; model S-4700, Hitachi, Canada) at an accelerating voltage of 2.0 kV.

Platelet Activation by Vascular Grafts

Platelet activation by the nonwoven PET structures (pristine and functionalized) and reference grafts were assessed by the use of Rhodamin fluorescent dye and P-selectin (tagged with FITC anti-human). Briefly, the isolated platelets were completed to 20 mL volume with EDTA- PGI_2 suspended in 5 mL EDTA- PGI_2 containing $10 \mu\text{g} \cdot \text{mL}^{-1}$ rhodamine (Sigma–Aldrich), followed by a 15-min incubation, PBS wash and centrifugation. The PPP suspended platelets were then adjusted to a 250×10^6 platelets mL^{-1} PRP concentration by adding PPP in PRP. The PET structures were washed in PBS, placed in 24-well plates, and supplemented with 1 mL of PRP on each sample. Samples were incubated in PRP for 1 h under gentle agitation followed by washing with a saline solution. The adhered platelets were fixed with 2% paraformaldehyde (Sigma–Aldrich). Non-specific binding sites were blocked with 1% w/v bovine serum albumin (BSA) (Sigma–Aldrich) and incubated with anti-human CD62P (BD Pharmingen, Canada), whereas FITC Mouse IgG1, κ (BD Pharmingen, Canada). The CD62P is specific for human P-selectin the FITC Mouse IgG1 was used as dyeing negative control. Samples were finally examined under a confocal microscope (Carl Zeiss LSM 510).

Platelet activation was also quantified through secreted P-selectin and thromboxan-B2 (TXB2) after 1 h platelet incubation (250×10^6 platelets mL^{-1}) with PET structures (pristine and functionalized) and reference grafts. The platelet suspension supernatants were quantified by the sP-selectin/CD62P kit (R&D systems) enzyme linked immunosorbent assay (ELISA) specific for P-selectin and TXB2 kit (Assay designs) specific for thromboxan-B2 (TXB2). For both the P-selectin and TXB2 ELISA assays the reagents, samples, and controls were diluted five times with the sample diluent supplied in the kit, and incubated with the appropriate conjugate during 1 h. The substrates were incubated for 15 min and its absorbance was measured at 450 nm. In both the P-selectin and TXB2 secretion evaluations negative and positive controls were added. The supernatant of platelets incubated in an empty well (i.e., without fiber structure) represented non-activated platelets and platelets incubated with thrombin receptor activated peptide-1 (TRAP-1) represented activated platelets, as positive control.

Endothelial Cell Adhesion

Human brain endothelial cells (HBEC) were obtained from small intracortical microvessels and capillary fractions (20–112 μm) harvested from human temporal cortex excised surgically from patients treated for idiopathic epilepsy. Tissues were obtained with approval from the Institutional Research Ethics Committee. HBEC were separated from SMC with cloning rings and grown in media containing Earle's salts, 25 mM 4-(2-hydroxyethyl)-1-piperazineethanesulfonic acid (HEPES), 4.35 $\text{g}\cdot\text{L}^{-1}$ sodium bicarbonate, and 3 mM L-glutamine, 10% FBS, 5% human serum, 20% of media conditioned by murine melanoma cells (mouse melanoma, Cloudman S91, clone M-3, melanin-producing cells), 5 $\mu\text{g}\cdot\text{mL}^{-1}$ insulin, 5 $\mu\text{g}\cdot\text{mL}^{-1}$ transferrin, 5 $\text{ng}\cdot\text{mL}^{-1}$ selenium, and 10 $\mu\text{g}\cdot\text{mL}^{-1}$ endothelial cell growth supplement.^[2] Cells were grown at 37 °C in humidified atmosphere of 5% CO_2 /95% air until reaching about 80% confluence. HBEC cultures were routinely characterized morphologically and biochemically. More than 95% of cells in culture stained immunopositive for the selective endothelial markers, angiotensin II-converting enzyme, and Factor VIII-related antigen, incorporated fluorescently labeled Ac-LDL, and exhibited high activities of the blood-brain barrier-specific enzymes, γ -glutamyltranspeptidase, and alkaline phosphatase.

PET fiber structures were sterilized in penicillin/streptomycin (200 U/200 $\mu\text{g}\cdot\text{mL}^{-1}$) for 3 h, washed three times with Hank's buffered salt solution (HBSS) and then pre-wetted in HBSS media overnight. Media was then removed and 50 μL of culture media containing 5×10^4 HBECs were applied to the scaffolds and allowed to sit for 20 min before filling up the wells with additional 450 μL of media. Cells were then incubated for 2 and 3 days at 37 °C in humidified atmosphere of 5% CO_2 /95% O_2 .

To visualize the cells and evaluate cell death, endothelial cells were washed twice with warm HBSS, incubated with 10 $\mu\text{g}\cdot\text{mL}^{-1}$ CFDA-AM (Molecular Probes, Frederick, MD, USA) at 37 °C for 45 min and then washed again with HBSS before nuclei counterstaining with 10 $\mu\text{g}\cdot\text{mL}^{-1}$ propidium iodide (Sigma, Oakville, ON) for 15 min at 37 °C in dark. Cells were then washed twice in HBSS and placed on glass slides. Microphotographs of the cells attached to the meshes were obtained using an Olympus 1 \times 50 microscope. Images were captured using a digital video camera (Olympus U-CMT) and analyzed with Northern Eclipse v.5.0 software.

Statistical Analysis

Results are represented as mean \pm standard deviation (SD). Statistical difference was analyzed using one-way analysis

of variance (ANOVA), and p -values <0.05 were considered significant.

Results and Discussion

Physicochemical Characteristics of Nonwoven PVA/PEG Functionalized PET Fibers Structures

Scanning electron microscopy (SEM) micrographs of the unmodified nonwoven PET fiber structures are shown in Figure 2 at low and high magnification. The commercial woven Dacron grafts morphology was also characterized and is shown in Figure 2. The nonwoven PET fiber structure differs considerably from the commercial woven grafts in many aspects. Apart from their nonwoven structure, their fiber size is also quite different, with the nonwoven structure being composed of fibers ranging between 3 and 8 μm in diameter. This contrasts from the commercial woven grafts made of monodispersed fibers of approximately 20 μm in size. In addition, and in the context of this study most importantly, pore size distribution differs significantly from a narrow 5 to 20 μm for our nonwoven structure to a bi-modal pore size distribution for the commercial Dacron woven grafts where small pore population relates to interfiber spacing (≈ 5 –10 μm) and large pore population relates to depression between fiber yarns (≈ 50 –100 μm). While the above described Dacron vascular grafts provide adequate pore size for tissue growth during the healing process, the fiber yarns (≈ 50 –100 μm) pore structure is sufficiently large to promote bleeding and red blood cells retention within the graft.^[3] Further, pore openings >20 μm in a graft usually promote collagenous tissue ingrowth rendering the graft inflexible.^[3] This large pore size disadvantage with Dacron vascular grafts is particularly acute during the initial healing stages after the implantation reducing satisfactory healing potential due to the bleeding potential. Despite the dense bovine collagen coating on the luminal surface of Dacron woven grafts the large inter-fiber yarns pores remain exposed.

The stepwise surface modification of PET fibers was confirmed via fluorescence by reacting the amino-modified fibers with fluorescamine which is intrinsically non-fluorescent but becomes highly fluorescent upon the reaction with primary amino groups (data not shown). In addition to this, the fibers were derivatized with Cy5 by reacting the corresponding NHS monofunctionalized Cy5 dye and the amino-modified fibers and subsequently visualizing them with a fluorescence microscope to confirm successful modification (data not shown). In addition to fluorescence imaging, the chemical modification steps were confirmed by XPS. Figure 3 and Table 2 illustrate the survey spectra and the relative atomic

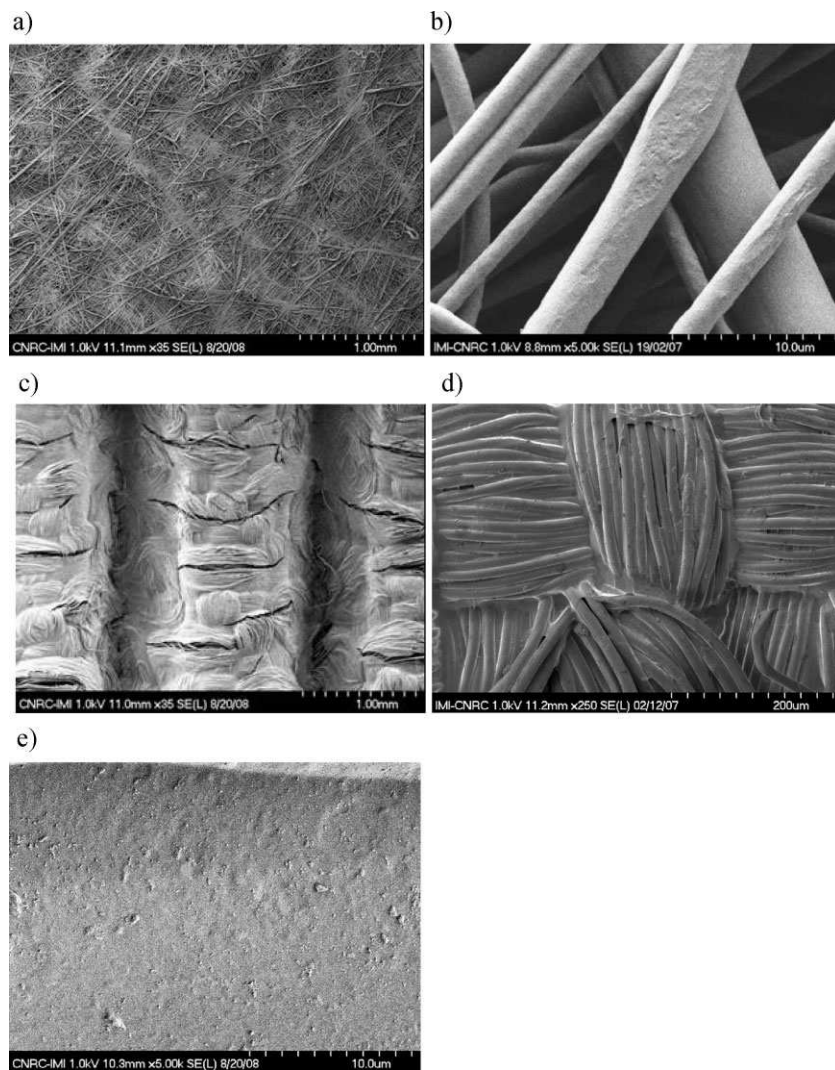


Figure 2. Scanning electron micrographs of pristine nonwoven PET fibre structures at low (a), high magnification (b), and of commercial bovine collagen-coated Dacron grafts (Hemashield Platinum, Woven Double Velour, and Boston Scientific) at low (c) medium (d) and high (e) magnification.

percentages at each modification step. The inset in Figure 3 depicts line deconvolutions of the high-resolution spectra from the line corresponding to C 1s. The atomic percentages for pristine fibers of PET do agree with their expected values within 2%. Line deconvolution of C 1s from the pristine fibers clearly indicates three lines at 284.6 eV (A), 286.5 eV (B), and 288.5 eV (C) which correspond to the aromatic carbons, $^*CH_2-O-C(=O)-Ph$ and $CH_2-O-^*C(=O)-Ph$, respectively. The most important feature from this data is the incremental amount of incorporated nitrogen during the chemical modification steps. A trace amount of nitrogen (1%) was detected on pristine PET fibers, however, a substantial increase (5.6%) is observed upon the modification with amino groups indicating successful grafting of polyvinylamine on

the surface of the fibers. Line deconvolution corroborates the appearance of a new peak at 285.7 eV which is due to $^*CH-NH_2$. The signal from $^*CH_2-CH-NH_2$ is most likely overlapping with line A. A new small signal at 287.3 eV (line E) is also observed and it is indicative of the formation of amide groups. The subsequent surface modification of the fibers with PEG is confirmed by the increase of atomic nitrogen (6.6%) due to the amide group in the PEG reagent and by the appearance of a new band at 286.2 eV (F) which is associated with $^*CH_2-O$ from the PEG moiety.

Reduction of Platelet Adhesion on Nonwoven PET Fiber Structures

Using freshly isolated platelets, their adhesion was investigated on pristine and PEG-modified nonwoven PET structures functionalized with solutions containing 5, 7.5, 10, and 15% PEG. Carbon-coated ePTFE and collagen (bovine) coated Dacron grafts were used as positive and negative controls, respectively. As shown in Figure 4, based on the ^{51}Cr labeled platelet count, the highest platelet adhesion was seen on the pristine structures and PET nonwoven scaffolds functionalized with a 5% PEG solution with roughly 30 300 and 26 400 adhered platelets mm^{-2} , respectively. An increase of 2.5% in the PEG concentration in solution (i.e., 7.5% PEG) demonstrated a two-fold reduction in the platelet adhesion count to 9300 adhered platelets mm^{-2} , a figure statistically similar to platelet adhesion levels on collagen-coated Dacron. Finally, functionalizations using 10 and 15% PEG solutions demonstrated low platelet adhesion numbers of 3900 and 3800 adhered platelets mm^{-2} , respectively, which statistically resembles the carbon-coated ePTFE. This indicates that 10% is the optimal PEG solution concentration as it yields the lowest platelet adhesion with the least amount of PEG usage. Both the pristine and nonwoven PET structures modified with a 10% PEG solution were incubated with Mepacrine stained platelets for further characterization. As shown in Figure 5, the neat nonwoven PET fibers surface is covered with a continuous monolayer of platelets, while the PEG-modified nonwoven PET fibers support only scarce platelets adhesions. This is in

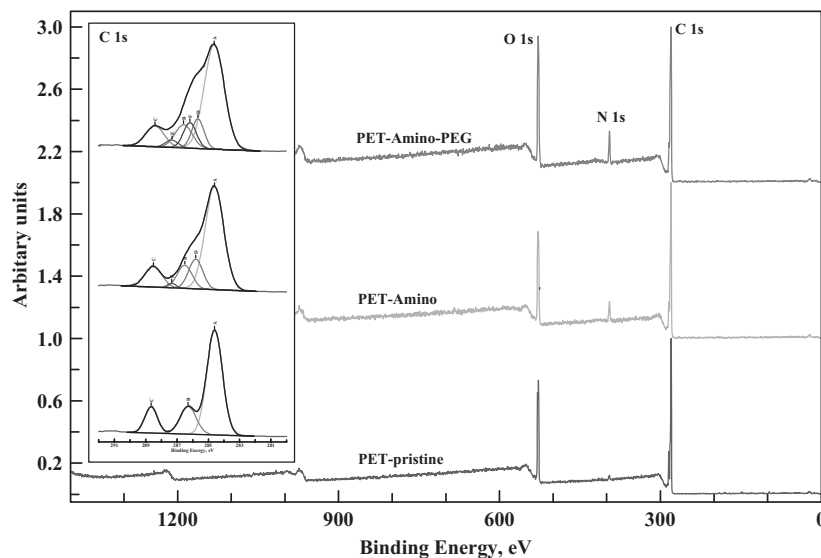


Figure 3. XPS spectra of pristine, amino-modified, and PEG-modified PET fibers illustrating the sequential increase of nitrogen content during the surface treatments. Inset set of spectra depicts line deconvolutions for C 1s and they corroborate the presence of PVA, the formation of amide linkages, and the grafting of 10% PEG.

agreement with the previously discussed platelet ^{51}Cr radioactive count.

On synthetic materials, platelet adhesion is mediated by plasma protein adsorption, specifically the adsorbed fibrinogen and von Willebrand factor.^[22] The effectiveness of a surfactant polymer coating in preventing protein and platelets adhesion is easily measured under static conditions considered as a “worst case” scenario allowing the prolonged undisturbed formation of platelet–surface interactions.^[7] The modification with 10% PEG solution incorporates enough hydrophilic chain molecules in the PET nonwoven grafts resulting in a seven-fold decrease platelets adhesion to the level of negative control, i.e. carbon-coated ePTFE (Figure 4), allows to conclude that the surface modification using a 10% PEG solution is sufficient in terms of anti-adhesion platelets effect. However these interpretations are based on 1 h platelets-structures incubation end point and the short incubation may be underestimating the long-term

Table 2. Surface atomic concentrations of C, O, and N on pristine, PVA- and PEG-modified nonwoven fibers as determined by XPS.

| | PET | PET-PVA | PET-PVA-PEG |
|------|------|---------|-------------|
| | % | % | % |
| C 1s | 72.6 | 69.4 | 66.8 |
| O 1s | 26.5 | 25.0 | 26.6 |
| N 1s | 1.0 | 5.6 | 6.6 |

effects of the structures on whole blood dynamic and therefore platelets activation processes.

Reduction of Platelet Activation on Nonwoven PET Fiber Structures

It is important to note that although some surfaces may not support significant platelet adhesion, they could potentially still activate platelets.^[9] Activated platelets release their granule contents, initiating a cascade attracting more platelets and show a typical shape change in the process. The morphological state is characterized by five stages indicative of the platelets activation: (I) round or discoid; (II) dendritic or early pseudopodial; (III) spread dendritic or intermediate pseudopodial; (IV) spreading or late pseudopodial; and (V) fully spread.^[17] To this end, the morphology of platelets co-incubated with PEG-functionalized (5% and 10% PEG

solutions) and pristine nonwoven PET fiber structures were studied by SEM (Figure 6). On pristine nonwoven PET fibers, platelets were well spread with well-developed pseudopodia, showing typical morphologies of activated state V. On the other hand, the nonwoven PET fibers functionalized with 10% PEG solution, yielded a remarkable suppression of platelets adhesion with neither pseudopodia extension nor platelets deformation. This morphology is typical of inactivated states of platelets, or state I as described above. The in-between

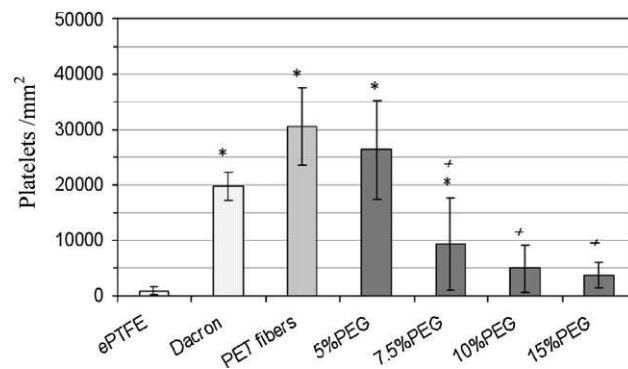


Figure 4. Platelet adhesion on two commercial structures, ePTFE and woven Dacron and on pristine, and PEG-modified nonwoven PET fibers that were functionalized with solutions containing 5, 7.5, 10, and 15% PEG. The platelets were labeled with ^{51}Cr and counted visually. The symbol * indicates significantly different standard deviation from ePTFE ($p < 0.05$) and # significantly different standard deviation from Dacron ($p < 0.05$).

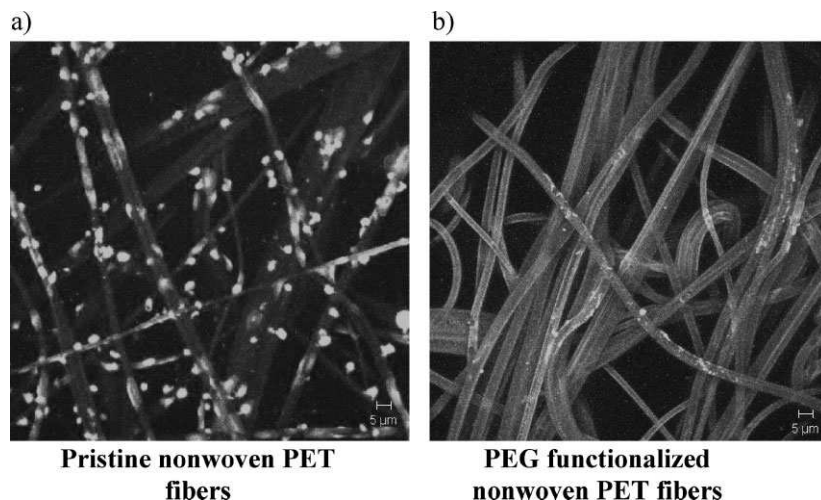


Figure 5. Platelet adhesion on a) pristine and b) nonwoven PET structures functionalized with a 10% PEG solution. Platelets were stained with Mepacrine dye. Original magnification was 200X.

nonwoven PET fibers functionalized with a 5% PEG solution demonstrated, as expected, some platelets aggregation and pseudopodia formation but far less spreading than pristine PET fibers. Therefore the morphological state of platelets on the nonwoven PET

fibers functionalized with a 10% PEG solution classified as early dendritic at worst shows greatly improved anti-thrombogenicity. In addition to the morphological changes as previously observed, the activation of platelets also leads to a release reaction of biochemical co-factors. Upon activation, and the above described cell shape change, platelet-platelet contact and adhesion are promoted leading to the release of their intracellular granular contents, including P-selectin. P-selectin is translocated from the α -granules of platelets to the membrane surface upon activation, making it a useful tool in assessing platelet activation of adhered platelets to the biomaterial.^[4] Therefore, the activation of platelets on the PEG-modified nonwoven PET fibers (using 10% PEG solution) was qualitatively characterized by rhodamine and human platelet P-selectin-FITC fluorescence markings. As seen in Figure 7, the scarcely adhered platelets on the PEG-modified nonwoven PET fibers did not demonstrate concurrent rhodamine and P-selectin markings indicating a low platelets activation level. The pristine nonwoven PET fibers on the other hand presented dense platelets adhesion with some concurrent rhodamine and P-selectin markings indicating activated platelets. However non-adhered platelets can also be activated based on their microenvironment and release their biologically active compounds stored in intracellular platelet granules into the microenvironment. In other words, in highly activated platelets, P-selectin is released, initiating the eicosanoid pathway, resulting in the liberation of thromboxane B₂ (TXB₂). A soluble form of P-selectin (sP-selectin) found in the plasma serves as a reliable marker of platelet activation and takes into account activated, yet unbound platelets to the exposed biomaterial.^[4,9] Therefore the secreted TXB₂ and sP-selectin levels were measured in the medium from co-cubated platelets with pristine, PEG-grafted nonwoven PET structures (5 and 10% PEG solutions) and the respective positive and negative controls: ePTFE and collagen (bovine) coated Dacron. As shown in Figure 8 no significant

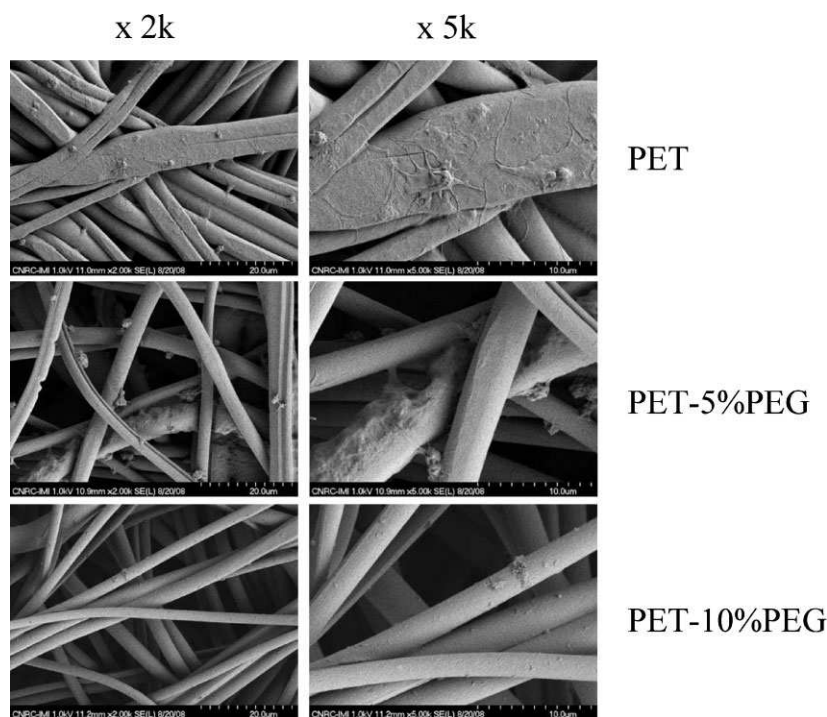


Figure 6. Platelet adhesion on pristine (top), nonwoven PET structures functionalized with 5% (middle) and 10% (bottom) PEG solutions, visualized through scanning electron microscopy (SEM) at low 2X (left hand side) at high 5X (right hand side) magnifications.

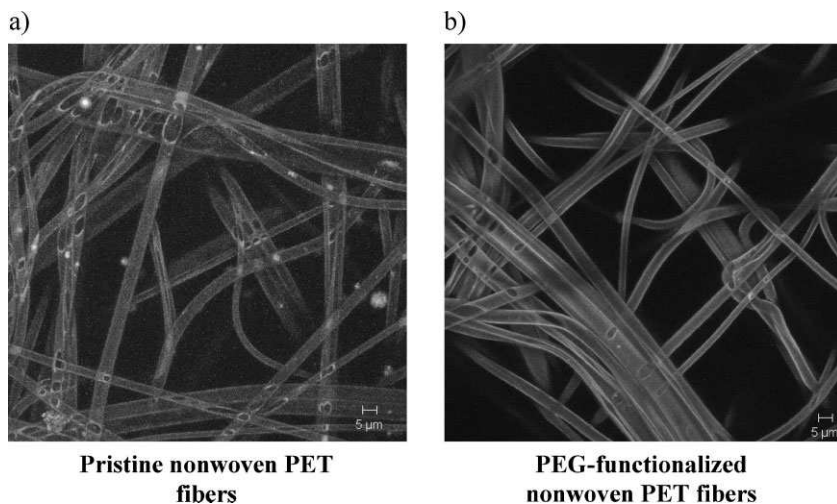


Figure 7. Platelet adhesion on a) pristine and b) nonwoven PET structures functionalized with 10% PEG solution. Platelets were stained with rhodamine (red) and P-selectin (green). The platelets are distinguishable as pale yellow structures attenuating the strong background fluorescence of the PET structures and are especially visible on the pristine structures. Original magnification was 200X.

biomaterials platelets activating potential as the lack of leukocytes restricts the activation of the coagulation cascade. Further studies with whole blood interactions are underway in our laboratory to elucidate the activation cascade of platelets in the presence of pristine, and PEG-grafted nonwoven PET structures for more conclusive results. It is also possible that 1 h incubation of platelets is simply not sufficient to generate detectable sP-selectin and TXB2 levels, and longer incubation times are needed to assess this effect.

Cell Adhesion

As shown in Figure 9, HBEC grew and adhered uniformly on both pristine PET and aminated nonwoven PET fibers.

However, HBEC plated on PEG-functionalized nonwoven PET grafts appeared sparsely distributed on the surface, forming aggregates in small areas. Furthermore, the cell number was progressively smaller with increasing time (3 versus 2 days) and percent of PEG-immobilized on the grafts. No significant cell death, represented by PI cell staining (red), was observed in either neat or aminated nonwoven PET grafts. In contrast, many cells in the PEG-functionalized fibers were PI-labeled, especially those located in the core of the cell aggregates. This is indicative of a reduced cell capacity to adhere on the PEG-functionalized PET fibers leading to cells detachment and death. Endothelial cell survival is known to be dependent on integrin-mediated cell attachment to basement membrane, which may explain that PI cell staining was more prominent on the PEG-modified structures where HBEC present reduced adhesion capacity.^[25] Although PEG functionalization appears to reduce endothelial cell adhesion to nonwoven PET surfaces, this does not hamper the main goal of its use in this study which is to prevent platelet attachment and thrombogenesis in the absence of the naturally occurring anti-thrombogenic endothelial cell layer.

Conclusion

Different loadings of PEG were incorporated into proprietary nonwoven PET scaffolds for 3D vascular grafts. Based on the PEG surface coverage as well as in vitro platelets adhesion, morphology and activation results, it can be concluded that functionalization of PET nonwoven fibers using a 10% PEG solution yields sufficient coverage to render the structures non-thrombogenic in vitro in the

differences in sP-selectin and TXB2 levels were observed among the neat, PEG-functionalized nonwoven PET fibers, and controls. These results suggest that in 1 h overall platelets are not activated even when co-incubated with pristine PET, which at first appears contradictory with results previously shown. However, it has been shown in literature that in adsorption studies on biomaterial surfaces with isolated plasma, the intrinsic and extrinsic pathway in material thrombosis does not activate in a representative manner of the physiological blood flow interaction.^[23] In fact, a study by Hong et al.^[24] suggested that the presence of leukocytes is required for activation of the coagulation cascade; the requirement of a TF-dependent pathway of initiation of coagulation may thus also apply to biomaterials. As the study was performed with isolated platelets and not whole blood it is possible that the TXB2 and sP-selectin levels secreted are not representative of the

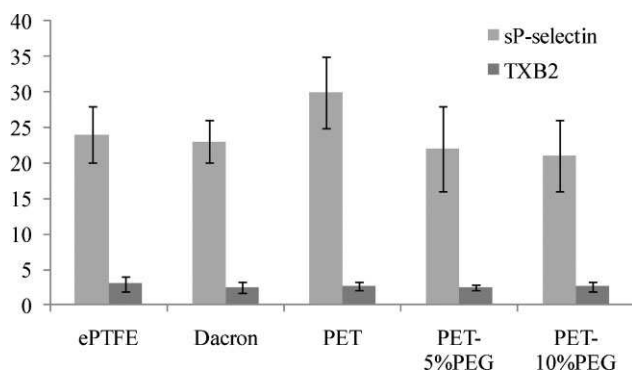


Figure 8. Dosage of sP-selectin and TXB2 expression in the supernatants of pristine nonwoven PET structures, PEG-functionalized with 5% PEG, and 10% PEG solutions in addition to ePTFE and woven Dacron controls, after 1 h of platelet incubation.

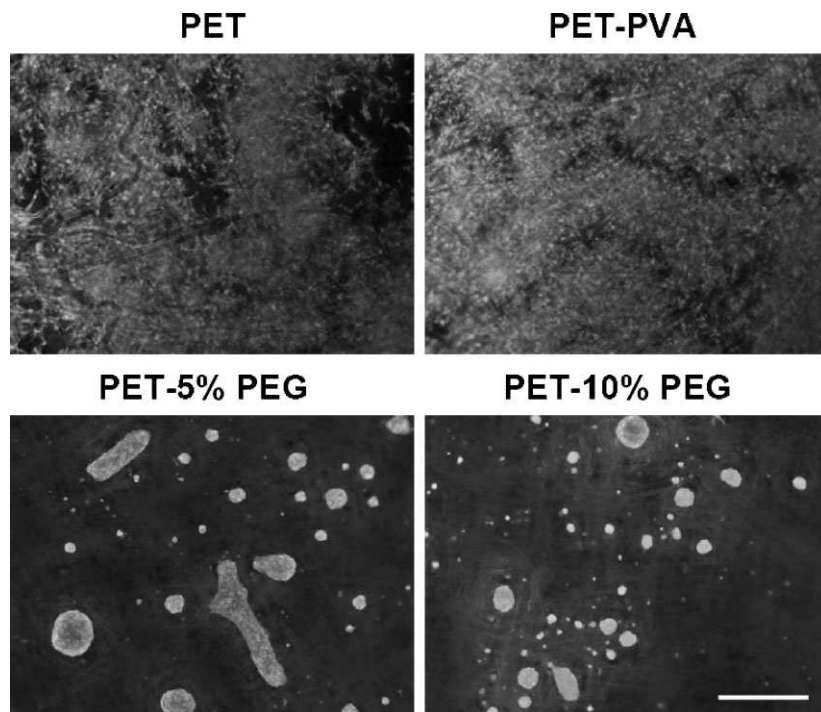


Figure 9. Representative micrographs illustrating the adhesion of human brain endothelial cells (CFDA, green) to pristine, amino-modified (PET-PVA), and PEG-modified (5 and 10% PEG solutions) nonwoven PET scaffolds. Cell death was evaluated by nuclei counterstaining with propidium iodide (red). Scale bar represents 400 μm for all images.

absence of the naturally occurring anti-thrombogenic endothelial cell layer. The relevance to small diameter vascular grafts replacements of our stable under shear stress PEG-coating is based on our PEG coating high reduction of non-specific protein adsorption mediated by the reduction of plasma protein adsorption. These PEG-coated nonwoven PET structures have the advantages of (1) being based on a well-known and accepted polymer in the vascular prosthesis field, (2) showing artery-matching compliance, and (3) having a highly biostable and minimally thrombogenic off-the-shelf coating.

Acknowledgements: The help of *Nathalie Raymond* with the scaffolds functionalization, and *Francois Vachon, Jacques Dufour* with the scaffold fabrication (*National Research Council Canada*) and the financial support of the *Natural Sciences and Engineering Research Council of Canada (NSERC)* and of the *Biomedical Science and Technology Research Group (GRSTB)*, funded by the *Fonds de la recherche en santé du Québec (FRSQ)*, are gratefully acknowledged.

Received: September 21, 2010; Revised: November 24, 2010;
Published online: January 21, 2011; DOI: 10.1002/mabi.201000390

Keywords: fibers; luminal side coating; monolayer; non-thrombogenic; PEG; PET; platelets; small diameter vascular grafts

- [1] N. L'Heureux, N. Dusserre, G. Konig, B. Victor, P. Keire, T. N. Wight, N. A. F. Chronos, A. E. Kyles, C. R. Gregory, G. Hoyt, R. C. Robbins, T. N. McAllister, *Nat. Med.* **2006**, *361*, 361–365.
- [2] M. J. Moreno, A. Ajji, D. Mohebbi-Kalhari, M. Rukhlova, A. Hadjizadeh, M. N. Bureau, *J. Biomed. Mater. Res. Part B*. (In press) JBMR-B-09-0495.
- [3] S. Sarkar, K. M. Sales, G. Hamilton, M. S. Seifalian, *J. Biomed. Mater. Res. Part B* **2006**, *82B*, 100.
- [4] M. B. Gorbet, M. V. Sefton, *Biomaterials* **2004**, *25*, 5681.
- [5] Q. Yongzhi, Z. Ning, K. Qian, A. Yuehuei, W. Xuejun, *J. Biomed. Mater. Res. Part B* **2009**, *90B*, 668.
- [6] G. Perego, P. Preda, G. Pasquinelli, T. Curti, A. Freyrie, E. Cenni, *J. Biomater. Sci., Polym. Ed.* **2003**, *14*, 1057.
- [7] C. Tang, F. Kligman, C. C. Larsen, K. Kottke-Marchant, R. E. Marchant, *J. Biomed. Mater. Res. Part A* **2009**, *88A*, 348.
- [8] W. Shuwu, A. S. Gupta, S. Sagnella, P. M. Barendt, K. Kottke-Marchant, R. E. Marchant, *J. Biomater. Sci. Polym. Ed* **2009**, *20*, 619.
- [9] D. Motlagh, J. Yang, K. Y. Lui, A. R. Webb, G. A. Ameer, *Biomaterials* **2006**, *27*, 4315.
- [10] P. Losi, S. Lombardi, E. Briganti, G. Soldani, *Biomaterials* **2004**, *25*, 4447.
- [11] S. Dimitrievska, M. Moreno, E. Pinney, R. Gendron, M. N. Bureau, *Proc. Soc. Biomater. Ann. Mtng.* Seattle, Washington, April 21 2010, STAR award.
- [12] S. Dimitrievska, A. Petit, A. Ajji, M. N. Bureau, L. Yahia, *J. Biomed. Mater. Res. Part B* **2008**, *1*, 44.
- [13] S. Sarkar, K. M. Sales, G. Hamilton, A. M. Seifalian, *J. Biomed. Mater. Res. Part B* **2006**, *82B*, 100.
- [14] Z. Gong, L. E. Niklason, *FASEB J* **2008**, *22*, 1635.
- [15] P. Macchiarini, P. Jungebluth, T. Go, M. Adelaide Asnaghi, L. E. Rees, T. A. Cogan, A. Dodson, J. Martorell, S. Bellini, P. Paolo Parnigotto, S. C. Dickinson, A. P. Hollander, S. Mantero, M. Teresa Conconi, M. A. Birchall, *Lancet* **2008**, *372*, 2023.
- [16] L. Brannon-Peppas, *J. Controlled Release* **2000**, *66*, 321.
- [17] F. Ryoko, H. R. D. Piwai, C. Wei, *J. Appl. Polym. Sci. Part A* **2004**, *42*, 5389.
- [18] S. Q. Liu, R. Tay, M. Khan, P. L. R. Ee, J. L. Hedrick, Y. Y. Yang, *Soft Mater* **2010**, *6*, 67.
- [19] D. S. W. Benoit, M. P. Schwartz, A. R. Durney, K. S. Anseth, *Nat. Mater.* **2008**, *7*, 816.
- [20] H. Abou-Saleh, D. Yacoub, J.-F. Théorêt, M.-A. Gillis, P.-E. Neagoe, B. Labarthe, P. Théroux, M. G. Sirois, M. Tabrizian, E. Thorin, Y. Merhi, *Circulation* **2009**, *120*, 2230.
- [21] Y. Merhi, M. King, R. Guidoin, *J. Biomed. Mater. Res.* **1997**, *34*, 477.
- [22] N. M. K. Lamba, S. L. Copper, *Hemostasis and Thrombosis, Basic Principles & Clinical Practices*, 1st ed. Lippincott Williams & Wilkins, Philadelphia PA 2001, p. 661.
- [23] Y. Qiu, N. Zhang, Q. Kang, Y. An, X. Wen, *J. Biomed. Mater. Res. Part B* **2009**, *90B*, 668.
- [24] J. Hong, K. Nilsson Ekdahl, H. Reynolds, R. Larsson, B. Nilsson, *Biomaterials* **1999**, *20*, 603.
- [25] R. C. Bates, L. F. Lincz, G. F. Burns, *Cancer Metastasis Rev.* **1995**, *14*, 191.